

Discovery of a Potent and Selective Sphingosine Kinase 1 Inhibitor through the Molecular Combination of Chemotype Distinct Screening Hits

Mark E. Schnute, Matthew D. McReynolds, Jeffrey Carroll, Jill E Chrencik, Maureen K. Highkin, Kaliapan Iyanar, Gina Jerome, John W. Rains, Matthew Saabye, Jeffrey A. Scholten, Matthew Yates, and Marek M. Nagiec

J. Med. Chem., **Just Accepted Manuscript** • DOI: 10.1021/acs.jmedchem.7b00070 • Publication Date (Web): 23 Feb 2017

Downloaded from <http://pubs.acs.org> on February 24, 2017

Just Accepted

“Just Accepted” manuscripts have been peer-reviewed and accepted for publication. They are posted online prior to technical editing, formatting for publication and author proofing. The American Chemical Society provides “Just Accepted” as a free service to the research community to expedite the dissemination of scientific material as soon as possible after acceptance. “Just Accepted” manuscripts appear in full in PDF format accompanied by an HTML abstract. “Just Accepted” manuscripts have been fully peer reviewed, but should not be considered the official version of record. They are accessible to all readers and citable by the Digital Object Identifier (DOI®). “Just Accepted” is an optional service offered to authors. Therefore, the “Just Accepted” Web site may not include all articles that will be published in the journal. After a manuscript is technically edited and formatted, it will be removed from the “Just Accepted” Web site and published as an ASAP article. Note that technical editing may introduce minor changes to the manuscript text and/or graphics which could affect content, and all legal disclaimers and ethical guidelines that apply to the journal pertain. ACS cannot be held responsible for errors or consequences arising from the use of information contained in these “Just Accepted” manuscripts.

1
2
3
4
5
6
7
8
9
10
11
12
13
14
15
16
17
18
19
20
21
22
23
24
25
26
27
28
29
30
31
32
33
34
35
36
37
38
39
40
41
42
43
44
45
46
47
48
49
50
51
52
53
54
55
56
57
58
59
60

Discovery of a Potent and Selective Sphingosine Kinase 1 Inhibitor through the Molecular Combination of Chemotype Distinct Screening Hits

*Mark E. Schnute**,[†] *Matthew D. McReynolds*,[†] *Jeffrey Carroll*,[†] *Jill Chrencik*,[§] *Maureen K. Highkin*,[‡] *Kaliapan Iyanar*,[†] *Gina Jerome*,[‡] *John W. Rains*,[‡] *Matthew Saabye*,[‡] *Jeffrey A. Scholten*,[†] *Matthew Yates*,[‡] and *Marek M. Nagiec*[‡]

[†]Medicine Design and [‡]Inflammation and Immunology Research, Pfizer, Cambridge, Massachusetts 02139, United States

[§]Medicine Design, Pfizer, Groton, Connecticut 06340, United States

KEYWORDS: Sphingosine kinase, SphK1, SphK2, sphingosine-1-phosphate, S1P, high throughput screening

ABSTRACT: Sphingosine kinase (SphK) is the major source of the lipid mediator and GPCR agonist sphingosine-1-phosphate (S1P). S1P promotes cell growth, survival and migration and is a key regulator of lymphocyte trafficking. Inhibition of S1P signaling has been proposed as a strategy for treatment of inflammatory diseases and cancer. Two different formats of an enzyme

1
2
3 based high-throughput screen yielded two attractive chemotypes capable of inhibiting S1P
4 formation in cells. The molecular combination of these screening hits led to compound **22a** (PF-
5
6 formation in cells. The molecular combination of these screening hits led to compound **22a** (PF-
7
8 543) with two orders of magnitude improved potency. Compound **22a** inhibited SphK1 with an
9
10 IC₅₀ of 2 nM and was more than 100-fold selective for SphK1 over the SphK2 isoform. Through
11
12 the modification of tail region substituents, the specificity of inhibition for SphK1 and SphK2
13
14 could be modulated yielding SphK1 selective, potent SphK1/2 dual, or SphK2 preferential
15
16 inhibitors.
17
18
19
20
21
22
23
24

25 INTRODUCTION

26
27
28 The sphingosine kinases (SphK) are a family of lipid kinases that are responsible for the
29 phosphorylation of sphingosine (**1a**) to afford sphingosine-1-phosphate (S1P, **1b**), Figure 1.¹
30 S1P is an important bioactive lipid signaling molecule that acts as an agonist to five specific G
31 protein-coupled receptors (S1PR1–5) as well as displaying intracellular secondary messenger
32 actions.² S1P has a wide range of biological functions including promotion of cellular
33 proliferation and survival, immune cell trafficking, stimulation of angiogenesis, and regulation of
34 vascular integrity.³⁻⁵ As a consequence, its production and function as part of the SphK–S1P–
35 S1PR axis has profound implications towards human disease in the fields of inflammatory
36 disorders, cardiovascular disease, and oncology.
37
38
39
40
41
42
43
44
45
46
47
48

49 Two isoforms of SphK are found in mammalian organisms, SphK1 and SphK2.^{6,7} SphK1 (42
50 kDa) is found primarily in the cytoplasm and the plasma membrane of erythrocyte, endothelial
51 and mast cells. On the other hand, SphK2 is larger (63 kDa) and localized to the endoplasmic
52 reticulum, nucleus, and mitochondria. SphK1 and SphK2 demonstrate redundancy in function
53
54
55
56
57
58
59
60

1
2
3 since *Sphk1*^{-/-} and *Sphk2*^{-/-} mice independently are healthy and fertile while elimination of both
4 genes is embryonically lethal.^{8,9} Marked differences however have been observed between the
5 two transgenic strains towards plasma S1P levels. *Sphk1*^{-/-} mice display significantly reduced
6 S1P levels (50%) in the plasma while *Sphk2*^{-/-} mice actually show S1P levels 3-4 fold higher
7 than wild type animals.^{8,10-12} The latter suggests a much more complex pharmacological role for
8 SphK2 than simply producing S1P, which has yet to be fully elucidated.

9
10
11
12
13
14
15
16
17
18 The therapeutic potential of targeting the S1P regulatory pathway has been best demonstrated
19 by the S1P1 receptor agonist fingolimod (FTY-720, 2-amino-2-(2-(4-octylphenyl)ethyl)-1,3-
20 propanediol).¹³ Fingolimod is a “functional antagonist” of the receptor since its binding leads to
21 receptor internalization and degradation, and agonist signaling through the S1P1 receptor by S1P
22 is required for lymphocyte egress in inflammatory disease. Efficacy in a variety of preclinical
23 autoimmune models has been reported for fingolimod through its ability to block this
24 signalling.¹³ In humans, fingolimod has been shown to induce lymphopenia and is approved for
25 the treatment of relapsing remitting multiple sclerosis.^{14,15}

26
27
28
29
30
31
32
33
34
35
36
37
38
39
40
41
42
43
44
45
46
47
48
49
50
51
52
53
54
55
56
57
58
59
60
Consequently, the reduction of circulating or tissue specific S1P levels through the inhibition
of SphK has also been envisioned to have the potential to impact disease. *Sphk1*^{-/-} mice were
reported to show decreased synovial inflammation in a TNF- α -induced arthritis model; however,
Sphk2^{-/-} mice displayed more severe disease in the same model suggesting a SphK1 inhibitor
may be preferred for the potential treatment of rheumatoid arthritis.^{16,17} *Sphk1*^{-/-} mice were also
reported to be less susceptible to colitis induced by dextran sodium sulfate (DSS), a preclinical
model of irritable bowel disease (IBD).¹⁸ S1P and SphK1 may also play a role in the
development of fibrosis.¹⁹ Expression of SphK1 negatively correlates with lung function and
survival for patients with idiopathic pulmonary fibrosis (IPF), and *Sphk1*^{-/-} mice were reported to

1
2
3 be protected from disease symptoms in the bleomycin model of fibrosis.²⁰ A two-fold elevation
4
5 of SphK1 has been reported in the livers of patients with non-alcoholic fatty liver disease
6
7 suggesting S1P may promote hepatic inflammation.²¹ In a preclinical model of non-alcoholic
8
9 steatohepatitis (NASH), *Sphk1*^{-/-} mice were protected from disease. Also, wild type diabetic
10
11 mice were reported to exhibit increased renal cortical S1P and renal fibrosis markers compared
12
13 to SphK1 deficient diabetic mice.²² In recent studies, inhibition of SphK1 ameliorated cardiac
14
15 hypertrophy and dysfunction in hypoxic models of myocardial infarction and pulmonary arterial
16
17 hypertension.^{23,24} SphK1 has been found to be overexpressed in many types of cancerous
18
19 tumors.²⁵⁻²⁷ S1P produced by SphK1 is believed to contribute to prosurvival and antiapoptotic
20
21 mechanisms as well as chemotherapy resistance. However, the translation of SphK inhibitors to
22
23 reduced cancer cell survival has not been straightforward.²⁸ Recently, S1P levels have been
24
25 reported to be elevated in the blood of mice and humans with sickle cell disease (SCD), and
26
27 SphK1 inhibition by an inhibitor or siRNA resulted in reduced cell sickling.²⁹

28
29
30
31
32
33
34 The evolution of SphK1 and SphK2 inhibitors has been recently reviewed.³⁰⁻³² Many SphK
35
36 inhibitors mimic the substrate (sphingosine, **1a**) in that they have a polar head group and a
37
38 lipophilic tail region. One such example is compound **2** reported by Genzyme to be a potent
39
40 SphK1 inhibitor (IC₅₀ = 58 nM), Figure 2.³³ The first co-crystal structure of SphK1 with an
41
42 inhibitor was reported by Amgen utilizing compound **3a** (SphK1 IC₅₀ = 20 nM, SphK2 IC₅₀ =
43
44 1.6 μM).³⁴ They also found that a related analog **3b** reduced plasma S1P levels when dosed
45
46 orally in mice. Researchers at the University of Virginia and Virginia Tech have reported a
47
48 series of amidine and guanidine-based SphK inhibitors represented by **4a** and **4b**.³⁵⁻³⁷
49
50
51
52
53
54
55
56
57
58
59
60
Compound **4b** was a potent inhibitor of SphK1 (IC₅₀ = 48 nM) while being highly selective for
SphK2 (IC₅₀ > 10 μM). On the other hand, removal of the methylene linker as in compound **4a**

1
2
3 afforded one of the most potent SphK2 selective compounds reported (SphK1 IC_{50} = 13 μ M,
4 SphK2 IC_{50} = 1.3 μ M). Efforts to decipher the complex pharmacology between SphK1 and
5
6 SphK2 will require a range of potent inhibitor tool compounds consisting of SphK1 selective,
7
8 SphK2 selective and SphK1/2 dual inhibitors. By employing high throughput screening
9
10 methodology, we have identified two SphK inhibitor chemotypes. Subsequent optimization
11
12 strategies including molecular combination of these two series was successful in identifying
13
14 highly potent SphK1 selective and SphK1/2 dual inhibitors as well as compounds favoring
15
16 SphK2 inhibition.
17
18
19
20
21
22
23
24
25

26 RESULTS AND DISCUSSION

27 28 29 **Screening Strategy**

30
31
32 In order to provide the broadest opportunity to identify SphK inhibitors, we screened the Pfizer
33
34 compound collection using two different formats of a recombinant enzyme assay. In one
35
36 approach, a screening subset (ca. 150 000 compounds) was screened for a compound's ability to
37
38 inhibit the production of FITC-S1P by purified human SphK1 using a microfluidic mobility-shift
39
40 separation system (Caliper Life Sciences).³⁸ In parallel, a Transcreener® ADP detection assay
41
42 based on fluorescent polarization derived from binding of a fluorescent ADP derivative to an
43
44 anti-ADP antibody was used to screen a second unique compound subset (ca. 400 000
45
46 compounds) for the inhibition of ADP formation resulting from the enzyme reaction.³⁸ Both
47
48 compound collections were a diverse subset of the larger Pfizer compound file. The selection of
49
50 the compound collection with respect to assay was based on the screening capacity of the
51
52 individual assay. Subsequent confirmation using a dose response in the corresponding assay
53
54
55
56
57
58
59
60

1
2
3 yielded approximately 800 compounds (0.5% hit rate) from the Caliper® assay screen and
4
5 approximately 350 compounds (0.09% hit rate) from the Transcreener® assay screen with an
6
7 $IC_{50} < 10 \mu M$. Representative compounds from each distinct hit set were then assayed in the
8
9 respective orthogonal assay revealing a poor translation between the two recombinant enzyme
10
11 assays. In addition, a diverse set of compounds identified through the Caliper® assay screen all
12
13 showed a similar potency shift with respect to increased enzyme concentration. Both of these
14
15 observations suggested a potentially high artifact rate from one or more of the screening
16
17 approaches. The necessity to replicate the lipid associated environment native to SphK1 function
18
19 in a recombinant enzyme system (e.g. high detergent concentrations) may have contributed to
20
21 these findings. Therefore, a more physiologically relevant cell based assay was considered to
22
23 further hit validation.
24
25
26
27
28

29 Head and neck carcinoma 1483 cells were found to demonstrate a high conversion rate of C_{17} -
30
31 sphingosine to C_{17} -S1P. Also, a high ratio of SphK1 to SphK2 mRNA (700x) in these cells
32
33 suggested that SphK1 was the dominant isoform of S1P production. Subsequent triage efforts
34
35 focused on hit series which demonstrated potency in both recombinant enzyme assay formats as
36
37 well as displaying the ability to inhibit C_{17} -S1P production in 1483 cells. Gratifyingly, this effort
38
39 identified two attractive hit chemotypes, one from each enzyme screening assay format, Figure 3.
40
41 The first chemotype, the “aminobenzimidazole” series represented by compound **12**, was
42
43 identified from the Caliper® assay format. The second chemotype, the “benzylpyrrolidine”
44
45 series represented by **20a**, was identified from the Transcreener® assay.
46
47
48
49
50
51
52
53
54
55
56
57
58
59
60

Aminobenzimidazole Series

The screening hit **12** was synthesized as described in Scheme 1 through a convergent route forming the ether bond as the pivotal step. The required phenol was prepared from 3-(bromomethyl)-5-methylphenylacetate (**5**) by nucleophilic displacement of the bromide by the sodium salt of phenylsulfonic acid to provide sulfone **6**. Phenol **7** was then obtained by basic hydrolysis of the acetate protecting group. Diamine **8** was condensed with 1,3-bis(*tert*-butoxycarbonyl)-2-methyl-2-thiopseudourea to provide the nitrogen-protected aminobenzimidazole **9**. The ester was then reduced to afford alcohol **10** which facilitated Mitsunobu coupling with phenol **7**. Compound **12** was then obtained after deprotection. Similarly, the corresponding benzimidazole **15** was prepared by alkylation of phenol **6** with alkylchloride **14** which was prepared from alcohol **13**, Scheme 2.

Compound **12** demonstrated similar potencies in both the Caliper® and Transcreener® recombinant enzyme assays ($IC_{50} = 1.4 \mu M$ and $1.7 \mu M$, respectively). Only modest potency was observed against SphK2 ($IC_{50} = 39.6 \mu M$). Compound **12** inhibited the production of C_{17} -S1P in 1483 cells ($IC_{50} = 180 \text{ nM}$) with no indication of cellular toxicity (MTT, $50 \mu M$). Excellent kinome selectivity was observed (90 kinases, $< 50\%$ inhibition, $10 \mu M$ dose), and the compound did not bind to representative S1P receptors (S1P1-3,5; $IC_{50} > 10 \mu M$). Unfortunately due to low solubility, attempts to provide evidence of direct binding of compound **12** to SphK1 through ITC measurements were unsuccessful. The amino-substituent on the benzimidazole was found to be essential for SphK inhibition since compound **15** demonstrated significantly reduced potency in both the recombinant enzyme and cellular assays ($IC_{50} = 48 \mu M$ and $27 \mu M$, respectively).

Benzylpyrrolidine Series

The screening hit **20a** and subsequent analogs were prepared as described in Scheme 3. The coupling of 4-bromo-2-fluoro-1-nitrobenzene with (4-formylphenyl)boronic acid afforded biaryl **17**. The amine functionality was next installed through reductive amination of the aldehyde with pyrrolidine or 2-(hydroxymethyl)pyrrolidine to provide intermediates represented by compound **18**. Benzimidazoles **20a-j** were then prepared by displacement of the fluorine with a corresponding primary alkylamine (H_2NR'), condensation with acetaldehyde and reductive ring closure.

We prepared all four diastereomers of the screening hit in stereodefined configurations and assessed their ability to inhibit SphK1 and SphK2, Table 1. Diastereomer **20a** was found to be the most potent isomer with similar inhibitory potency in both the SphK1 Caliper® and Transcreener® recombinant enzyme assays ($IC_{50} = 0.87 \mu M$ and $0.19 \mu M$, respectively). It was also a potent inhibitor of C_{17} -S1P production in 1483 cells ($IC_{50} = 0.081 \mu M$) and demonstrated excellent kinome selectivity (89 kinases, < 50% inhibition, $10 \mu M$ dose). The other three diastereomers (**20b-d**) all showed weaker potency in all three assays with similar rank ordering. The stereospecificity of kinase inhibition demonstrated between **20a** and **20d** provided strong support for validation of the hit as directly interacting with SphK1. This was further supported by evidence of direct binding of **20a** to SphK1 as measured through ITC ($K_d = 2.9 \mu M$) and a corresponding weaker affinity for **20b** consistent with the functional assays.

The influence of the benzimidazole nitrogen substituent on SphK1 potency was explored in analogs **20e-i**, Table 2. More hydrophobic substituents that were either isosteric (**20g**) or larger (**20e,f**) than the tetrahydrofuranylmethyl of **20a** showed a profound improvement in potency. The increased potency of **20e-g**, however, was offset by the increased lipophilicity of the

1
2
3 molecules as demonstrated by a reduction in the LIPE compared to compound **20a**, Table 2. On
4
5 the other hand, replacing the saturated ring by phenyl (**20h**) or reducing the size of the
6
7 substituent (**20i**) was detrimental to potency. As demonstrated by compound **20j**, the
8
9 hydroxymethyl substituent of the pyrrolidine ring was critical for SphK1 inhibition. Based on
10
11 the structure-activity relationship for these and other analogs in the series, a strong correlation
12
13 between inhibition of the recombinant enzyme and inhibition of C₁₇-S1P production in 1483
14
15 cells was observed ($R^2 = 0.924$, $n = 60$), Figure 4. This correlation provided further support that
16
17 compound **20a** and related analogs are acting through inhibition of SphK1 to result in cellular
18
19 suppression of S1P production.
20
21
22
23
24
25
26

27 **Lead-hopping through molecular combination**

28
29
30 It is tempting to consider the benzimidazole present in both **12** and **20a** as a common
31
32 substructure when aligning the two chemotypes. However, it is important to consider the
33
34 structure-activity learnings for each series along with the nature of the endogenous ligand,
35
36 sphingosine – a molecule with a polar amine head and lipophilic tail. For compound **20a**, the 2-
37
38 (hydroxymethyl)pyrrolidine group is assumed to mimic the aminoalcohol head of sphingosine
39
40 and the substituted benzimidazole represents the lipophilic tail consistent with the critical
41
42 contribution of both regions to potency of the molecule. ROCS alignment³⁹ of compounds **12**
43
44 and **20a** based on both shape and functional group chemistry suggested the aminoimidazole
45
46 fragment of **12** indeed represented the polar terminus, Figure 5. This proposal would be
47
48 consistent with the loss of potency observed in replacing the amino group by hydrogen (**15**). The
49
50 alignment suggested the possibility of combining the hydrophobic tail of **12**, i.e.
51
52
53
54
55
56
57
58
59
60

1
2
3 ((phenylsulfonyl)methyl)phenoxy, with the polar head group of **20a**, i.e. (1-benzylpyrrolidin-2-
4 yl)methanol, Figure 3. The resulting combination was compound **22a** (PF-543),^{38,40} Table 3.
5
6

7
8 Compound **22a** and related analogs based on this hypothetical combination were prepared as
9 shown in Scheme 4. A substituted phenol such as **7** was alkylated by 4-bromomethyl-
10 benzaldehyde, and the resulting aldehyde was then reacted with a corresponding amine under
11 reductive alkylation conditions. Indeed compound **22a**, the product of direct combination of **12**
12 and **20a**, was found to be a potent inhibitor of SphK1 in recombinant enzyme assays, Table 3.
13 Compared to compound **20a**, a 100-fold improvement in cellular potency for inhibition of C₁₇-
14 S1P production was obtained (IC₅₀ = 0.8 nM). Similarly, LIPE improved to 6.8 (ΔLIPE = 2.0)
15 since the partition coefficient remained comparable to **20a** (**22a**, measured LogD = 2.3).
16
17

18
19 Compound **22a** also inhibited the production of C₁₇-S1P in a human whole blood ex-vivo assay
20 (IC₅₀ = 20 nM).⁴¹ Excellent kinome selectivity was observed (90 kinases, <50% inhibition, 10
21 μM dose) including selectivity against SphK2 (130-fold). The corresponding enantiomer **22b**
22 showed reduced potency, however, several hydroxypyrrolidine analogs (**22c-f**) also were found
23 to be potent inhibitors of SphK1, Table 3. Both pyrrolidinol **22c** and pyrrolidindiol **22e**
24 demonstrated superior potency to **22a** while maintaining a comparably high level of SphK2
25 selectivity. As shown with compound **22g**, the pyrrolidine ring was not essential for SphK1
26 inhibition, however, SphK2 inhibition was more sensitive to this structural change.
27
28

29
30 The role of the substituents to the tail region was also investigated. Compounds were prepared
31 as previously described (Scheme 4) where the required phenol was either commercially available
32 or prepared as described in Scheme 5 (**25a-c**) from 1-(bromomethyl)-3-methoxybenzene by
33 displacement followed by demethylation. It was found that the methyl substituent of the phenyl
34 ring was not a significant determinant for SphK1 potency as demonstrated by compound **26a**
35
36
37
38
39
40
41
42
43
44
45
46
47
48
49
50
51
52
53
54
55
56
57
58
59
60

1
2
3 since it showed comparable potency to **22a** in all assays with only a modest reduction in SphK2
4 selectivity, Table 4. Replacement of the phenylsulfone by alkylsulfones as in **26b** and **26c**,
5
6 however, did have detrimental effects on SphK1 inhibition. Deviating from the sulfonyl
7
8 substituent in the tail region resulted in some remarkable changes in Sphk1/2 inhibition profiles,
9
10 Table 5. Replacement of the phenyl methylsulfone with alkyl groups such as cyclohexyl (**27a**)
11
12 and isopropyl (**27b**) or a heteroaryl group (**27c**) still maintained excellent SphK1 inhibition with
13
14 compound **27a** being the most potent compound identified in this study (HWB C₁₇-S1P IC₅₀ =
15
16 1.5 nM). However, compounds **27a-c** were now dual inhibitors of SphK1 and SphK2. Further
17
18 replacement of the group by phenylamide (**27d**) significantly reduced SphK1 inhibition (IC₅₀ =
19
20 9.8 μM) while SphK2 potency (IC₅₀ = 145 nM) was comparable to compound **26a**.
21
22
23
24
25
26

27 The recent co-crystal structure of compound **22a** with SphK1 reported by Elkins and
28
29 coworkers is informative towards rationalizing the SAR observations for these three chemotypes,
30
31 Figure 6a.⁴² Compound **22a** was found to bind in the SphK1 substrate pocket adopting a J-
32
33 shaped conformation. The polar 2-(hydroxymethyl)pyrrolidine head group was observed to
34
35 make hydrogen-bond contacts from both the nitrogen and oxygen atoms to D264 of SphK1. The
36
37 remainder of the molecule protruded into a hydrophobic tunnel with the central phenyl ring
38
39 forming a π-hydrophobic contact with L345 and the terminal phenyl ring of the sulfone
40
41 contacting F374 at the base of the pocket. Docking analysis utilizing the co-crystal structure
42
43 with **22a** suggests that aminobenzimidazole **12** adopts a similar bound conformation due to the
44
45 shared hydrophobic region with compound **22a**, Figure 6b. However, unoptimized interactions
46
47 between the polar head region and D264 likely leads to the observed diminished potency.
48
49
50
51 Similarly based on the docking analysis, benzimidazole **20a** may benefit from the optimized
52
53 contacts to D264 in the polar region while the rest of the molecule would be accommodated in
54
55
56
57
58
59
60

1
2
3 the hydrophobic tunnel, Figure 6c. As seen with **22a**, a hydrophobic contact between the
4 benzimidazole ring and L345 is proposed. The preference for hydrophobic substituents on the
5 benzimidazole ring and L345 is proposed. The preference for hydrophobic substituents on the
6 benzimidazole ring (**20e-g**) is consistent with maximization of hydrophobic contacts in the
7 pocket leading to F374. The loss of potency for compound **22b**, the enantiomer of **22a**, is
8 consistent with the importance of the hydrogen bond contact between D264 and the hydroxyl
9 group. Compound **22c** was actually more potent than **22a** and also demonstrated an
10 enantiospecific effect on inhibition. It is proposed in the case of **22c** and **22e-f** that a hydrogen
11 bond contact between the 3-hydroxy group on the pyrrolidine ring and S254 may compensate for
12 the hydrogen bond loss to D264. In the tail region, even though the co-crystal structure of **22a**
13 revealed that the methyl substituent to the central phenyl ring is nicely accommodated in a
14 hydrophobic pocket created by F259, removal of the methyl (**26a**) had a negligible impact on
15 SphK1 potency. Further support for the importance of a hydrophobic interaction with F374 was
16 demonstrated by truncation of the sulfone substituent to methyl (**26c**) leading to a significant loss
17 in potency.
18
19
20
21
22
23
24
25
26
27
28
29
30
31
32
33
34
35

36 The potent dual SphK1/2 inhibition by compounds **27a-c** or preferential SphK2 inhibition by
37 compound **27d** was at first glance more challenging to rationalize based on the reported bound
38 conformation of **22a**. For compound **27d**, if a similar bound conformation to **22a** was adopted,
39 the phenylamide would protrude into H397 consistent with the poor potency to SphK1; however,
40 the homologous residue in SphK2 is also histidine. The high SphK1 potency of **27a-c** is also
41 unexpected since the phenyl substituent would not be able to adequately fill the hydrophobic
42 pocket to reach F374. A proposed explanation for the apparent inconsistencies is that the
43 phenylether in the bound conformations of compounds **27a-d** has rotated 180° such that the
44 substituents now are positioned where the methyl substituent resides in the co-crystal structure of
45
46
47
48
49
50
51
52
53
54
55
56
57
58
59
60

1
2
3 **22a**. This conformation effectively avoids the deep hydrophobic pocket and the high affinity is
4 now driven by either π -hydrophobic or π - π interactions between the phenyl substituent and F259,
5
6 common to SphK1 and SphK2.
7
8
9

10 11 12 13 14 CONCLUSION

15
16
17 High-throughput screening against SphK1 using two different assay formats successfully
18 identified two structurally distinct inhibitor chemotypes represented by compounds **12** and **20a**.
19
20 A lead-hopping strategy based on the combination of molecular fragments from these hits
21 resulted in the design of compound **22a** and the realization of a 100-fold improvement in SphK1
22 cellular potency in one step from the screening hits. In addition, compound **22a** demonstrated
23 high SphK1 selectivity against the SphK2 isoform as well as other kinases. On the other hand,
24 highly potent SphK1/2 dual and SphK2 preferential inhibitors were afforded from the same
25 chemotype by tuning the tail region of the molecule. The availability of potent inhibitors
26 displaying a range of SphK1/2 selectivity – SphK1, SphK1/2 dual or SphK2 – will be valuable
27 tools to interrogate the complex physiological roles played by the sphingosine kinase family.
28
29
30
31
32
33
34
35
36
37
38
39
40
41
42
43

44 EXPERIMENTAL SECTION

45
46
47 **General Methods.** All reagents and solvents were used as purchased without further
48 purification. The purity of the final compounds was characterized by high-performance liquid
49 chromatography (HPLC) using a gradient elution program (A: C18 column, acetonitrile/water,
50 5/95–100/0, 9 min, 0.05% trifluoroacetic acid; or B: C18 column, acetonitrile/water, 10/90–
51 80/20, 8 min, 0.05% trifluoroacetic acid) and UV-detection (220 nM). The purity of all final
52
53
54
55
56
57
58
59
60

1
2
3 compounds was 95% or greater. Proton (^1H) NMR chemical shifts are referenced to a residual
4 solvent peak.
5
6

7
8 **PAINS.** All active compounds have been electronically filtered for structural attributes
9 consistent with classification as pan assay interference compounds (PAINS) and were found to
10 be negative.⁴³ Compounds **12**, **20a** and **22a** have undergone broad kinase profiling and been
11 found not to be promiscuous (see supporting information).
12
13
14

15
16
17 **3-Methyl-5-(phenylsulfonylmethyl)phenyl acetate (6).** A suspension of 3-(bromomethyl)-5-
18 methylphenyl acetate⁴⁴ (108 g, 0.44 mol), NaSO_2Ph (80.2 g, 0.48 mol) and Aliquat® 336 (3.6 g,
19 8 mmol) was stirred at 85 °C for 18 hours and another 12 hours at room temperature. The
20 reaction mixture slurried in ethyl acetate, filtered through Celite®, and the filtrate was
21 concentrated. The crude product was purified by silica gel chromatography (hexane/EtOAc, 4/1)
22 to afford 60 g (45%) of **6** as a viscous liquid. MS (ES+) m/z 322 (M+NH₄). ^1H NMR (400 MHz,
23 CDCl₃) δ 7.65–7.44 (m, 5H), 6.73(bs, 1H), 6.64 (bs, 1H), 4.23 (s, 2H), 2.23–2.24 (s, 6H).
24
25
26
27
28
29
30
31
32
33

34 **3-Methyl-5-(phenylsulfonylmethyl)phenol (7).** A suspension of **6** (60 g, 0.20 mol), methanol
35 (375 mL), water (190 mL) and saturated aqueous sodium bicarbonate (190 mL) was stirred at
36 room temperature for 36 hours. Volatiles were removed in vacuo, and the residue was acidified
37 to approximately pH 2 using 6.0 N aqueous HCl (100 mL). The mixture was extracted with
38 EtOAc (2 × 500 mL). The combined organic layers were washed with water (2 × 100 mL)
39 followed by brine (100 mL), dried (Na_2SO_4), and concentrated. The residue was purified by
40 silica gel chromatography (hexane/EtOAc, 6/4) to afford 35 g (67%) of **7** as a white solid. MS
41 (ES+) m/z 280 (M+NH₄). ^1H NMR (400 MHz, CDCl₃) δ 9.30 (s, 1 H), 7.73–7.57 (m, 5 H), 6.51
42 (br. s, 1H), 6.40 (br. s, 1 H), 6.32 (br. s, 1 H), 4.49 (s, 2 H), 2.10 (s, 3 H).
43
44
45
46
47
48
49
50
51
52
53
54
55
56
57
58
59
60

1
2
3 **Methyl 2-((*tert*-butoxycarbonyl)amino)-1*H*-benzo[d]imidazole-5-carboxylate (9).** 1,3-
4
5 Bis(*tert*-butoxycarbonyl)-2-methyl-2-thiopseudourea (1.75 g, 6.0 mmol) was added to a solution
6
7 of methyl 3,4-diaminobenzoate (1.0 g, 6.0 mmol) in methanol (20 mL). The mixture was heated
8
9 at reflux for 3 h and then allowed to cool to room temperature. The reaction mixture was diluted
10
11 with Et₂O (10 mL) and filtered. The solids were washed with Et₂O (2 x 5 mL) and dried to
12
13 afford 365 mg (21%) of **9** as a solid. MS (ES+) *m/z* 292 (M+H). ¹H NMR (400 MHz, DMSO-*d*₆)
14
15 δ 12.15 (br. s., 1H), 11.19 (br. s., 1H), 8.02 (br. s., 1H), 7.73 (dd, *J*=8.4, 1.8 Hz, 1H), 7.45 (d,
16
17 *J*=8.2 Hz, 1H), 3.84 (s, 3 H), 1.45 - 1.64 (m, 9 H).
18
19
20
21

22 ***tert*-Butyl (5-(hydroxymethyl)-1*H*-benzo[d]imidazol-2-yl)carbamate (10).** A suspension of
23
24 **9** (10.5 g, 36 mmol) in CH₂Cl₂ (300 mL) was cooled to -78 °C and then a solution of DIBAL
25
26 (1.0 M in toluene, 180 mL) was added by addition funnel over a period of 2 h. The reaction
27
28 mixture was stirred at -78 °C overnight and then slowly warmed to room temperature. After 4 h,
29
30 the reaction mixture was diluted with ether, cooled to 0 °C, and quenched with water (25 mL)
31
32 and 15% aq. NaOH (7 mL). The organic layer was decanted and the residue was repeatedly
33
34 extracted with EtOAc (1.5 L). The combined organic layer was dried (Na₂SO₄) and concentrated
35
36 to afford 8.3 g (87%) of **10** as a solid. MS (ES+) *m/z* 264 (M+H).
37
38
39
40

41 ***tert*-Butyl (5-((3-methyl-5-((phenylsulfonyl)methyl)phenoxy)methyl)-1*H*-**
42
43 **benzo[d]imidazol-2-yl)carbamate (11).** Polymer supported triphenylphosphine (698 mg, 1.50
44
45 mmol), **7** (262 mg, 1.00 mmol), and **10** (316 mg, 1.20 mmol) were suspended in THF (16 mL).
46
47 Di-*tert*-butyl azodicarboxylate (345 mg, 1.50 mmol) was added. The mixture was allowed to
48
49 warm to room temperature and stir for 18 h. The reaction mixture was filtered and the resin
50
51 washed with THF (20 mL). The filtrate was concentrated. The crude product was purified by
52
53 column chromatography (Biotage 40M, heptane/EtOAc, 2/1 x 0.5 L; 1/1 x 0.5 L; EtOAc/MeOH,
54
55
56
57
58
59
60

1
2
3 100/0 x 0.5 L; 98/2 x 0.5 L) to afford 137 mg (27%) of **11** as a tan solid. MS (ES+) m/z 508
4
5 (M+H). ^1H NMR (400 MHz, DMSO- d_6) δ 11.83 (br. s., 1 H), 10.93 (br. s., 1 H), 7.75–7.70 (m, 3
6
7 H), 7.63–7.57 (m, 2 H), 7.41 (br. s., 1 H), 7.37 (d, $J=8.2$ Hz, 1 H), 7.08 (dd, $J=8.2, 1.2$ Hz, 1 H),
8
9 6.81–6.78 (m, 1 H), 6.55–6.51 (m, 2 H), 4.94 (s, 2 H), 4.57 (s, 2 H), 2.18 (s, 3 H), 1.52 (s, 9 H).

10
11
12 **5-((3-Methyl-5-((phenylsulfonyl)methyl)phenoxy)methyl)-1H-benzo[d]imidazol-2-amine**
13
14 (**12**). Trifluoroacetic acid (1 mL) was added to a solution of **11** (130 mg, 0.26 mmol) in CH_2Cl_2
15
16 (1 mL). The mixture was shaken for 1 h and then concentrated in a stream of nitrogen to afford a
17
18 yellow foaming solid. The solid was dissolved in acetonitrile/THF and passed through a
19
20 Stratosphere PS- CO_3 cartridge eluting with additional methanol. The filtrate was concentrated
21
22 and purified by reverse-phase preparative HPLC to afford 23.8 mg (23%) of **12**. MS (ES+) m/z
23
24 408 (M+H). ^1H NMR (400 MHz, DMSO- d_6) δ 10.67 (br. s., 1 H), 7.75–7.67 (m, 3 H), 7.61–7.55
25
26 (m, 2 H), 7.13–7.03 (m, 2 H), 6.87 (d, $J=8.1$ Hz, 1 H), 6.76 (s, 1 H), 6.50 (s, 2 H), 6.15 (s, 2 H),
27
28 4.86 (s, 2 H), 4.55 (s, 2 H), 2.16 (s, 3 H).
29
30
31
32
33

34 **tert-Butyl 5-(chloromethyl)-1H-benzo[d]imidazole-1-carboxylate (14)**. Polymer-supported
35
36 Ph_3P (448 mg, 0.8 mmol) was added to a solution of *tert*-butyl 5-(hydroxymethyl)-1H-
37
38 benzo[d]imidazole-1-carboxylate (100 mg, 0.4 mmol) in CCl_4 (10 mL). The mixture was stirred
39
40 for 1 h and then was filtered. The filtrate was dried (MgSO_4), filtered and concentrated to afford
41
42 80 mg (74%) of **14**. MS (ES+) m/z 211 (M-*t*Bu+H).
43
44
45

46 **5-((3-Methyl-5-((phenylsulfonyl)methyl)phenoxy)methyl)-1H-benzo[d]imidazole (15)**. A
47
48 mixture of **14** (51 mg, 0.19 mmol), **7** (50 mg, 0.19 mmol), and potassium carbonate (106 mg,
49
50 0.76 mmol) in acetone (6 mL) was heated at 65 °C overnight. The reaction mixture was
51
52 concentrated and purified by reverse-phase preparative HPLC. The eluent was neutralized with
53
54 sodium bicarbonate and extracted with EtOAc. The organic layer was concentrated, and then the
55
56
57
58
59
60

1
2
3 residue was dissolved in CH₂Cl₂ (5 mL). The solution was cooled to 0 °C and trifluoroacetic
4
5 acid (1 mL) was added. The reaction mixture was stirred for 4 h and then passed through a
6
7 StratoSpheres® PL-HCO₃ MP cartridge. The filtrate was concentrated and lyophilized to afford
8
9 20 mg (27%) of **15** as a white solid. MS (ES+) m/z 393 (M+H). ¹H NMR (600 MHz, DMSO-*d*₆)
10
11 δ 9.13 (br. s., 1H), 7.82–7.76 (m, 2H), 7.75–7.68 (m, 3H), 7.62–7.55 (m, 2H), 7.50 (d, *J*=8.52
12
13 Hz, 1H), 6.83 (s, 1H), 6.62 (s, 1H), 6.54 (s, 1H), 5.14 (s, 2H), 4.56 (s, 2H), 2.19 (s, 3H).
14
15
16

17 18 **Representative synthesis of compounds 20a-j.**

19
20 **3'-Fluoro-4'-nitro-[1,1'-biphenyl]-4-carbaldehyde (17).** A solution of (4-formylphenyl)-
21
22 boronic acid (8.62 g, 57.4 mmol), 2-(dicyclohexylphosphino)biphenyl (0.33 g, 0.94 mmol),
23
24 Pd(OAc)₂ (0.11 g, 0.49 mmol), KF (8.7 g, 150 mmol) and 4-bromo-2-fluoro-nitrobenzene (11.0
25
26 g, 50 mmol) in dioxane (114 mL) was degassed three times and then heated at 65 °C for 18 h.
27
28 The reaction mixture was diluted with EtOAc and filtered through Celite®. The filtrate was
29
30 concentrated and the residue was purified by silica-gel column chromatography (petroleum
31
32 ether/EtOAc, 8/2) to afford 7.12 g (58%) of **17** as a yellow solid. MS (APCI) m/z 245 (M+). ¹H
33
34 NMR (400 MHz, CDCl₃) δ 10.18 (s, 1H), 8.21 (t, *J*=7.8 Hz, 1H), 8.02 (d, *J*=8.2 Hz, 2H), 7.77 (d,
35
36 *J*=8.2 Hz, 2H), 7.55 (d, *J*=8.6 Hz, 2H).
37
38
39

40
41 **(R)-(1-((3'-fluoro-4'-nitro-[1,1'-biphenyl]-4-yl)methyl)pyrrolidin-2-yl)methanol (18, NR₂**
42
43 **= (R)-pyrrolidin-2-ylmethanol).** Sodium triacetoxyborohydride (2.04 g, 9.63 mmol) was added
44
45 to a solution of **17** (1.41 g, 5.73 mmol) in 1,2-dichloroethane (50 mL). (*R*)-2-(hydroxymethyl)-
46
47 pyrrolidine (0.50 mL, 5.0 mmol) was added drop wise to the solution over 10 min. The mixture
48
49 was stirred at room temperature for 2 h and then saturated aqueous sodium bicarbonate solution
50
51 (50 mL) was added. The organic layer was separated, dried (MgSO₄), filtered and concentrated.
52
53
54
55 The residue was purified by silica-gel column chromatography (CH₂Cl₂/methanol, 90/10) to
56
57
58
59
60

1
2
3 afford 1.62 g (98%) of **18** as a yellow oil. MS (ES+) m/z 331 (M+H). ^1H NMR (400 MHz,
4
5 CDCl_3) δ 8.20–8.12 (m, 1H), 7.60–7.54 (m, 2H), 7.54–7.42 (m, 4H), 5.30 (s, 1H), 4.04 (d,
6
7 $J=13.3$ Hz, 1H), 3.69 (dd, $J=10.7, 3.5$ Hz, 1H), 3.51–3.41 (m, 2H), 3.06–2.97 (m, 1H), 2.83–2.74
8
9 (m, 1H), 2.38–2.28 (m, 1H), 2.04–1.81 (m, 2H), 1.80–1.67 (m, 2H).

10
11
12 **((R)-1-((4'-Nitro-3'-(((R)-tetrahydrofuran-2-yl)methyl)amino)-[1,1'-biphenyl]-4-**
13
14 **yl)methyl)pyrrolidin-2-yl)methanol (19, NR₂ = (R)-pyrrolidin-2-ylmethanol). (R)-2-**
15
16 (Aminomethyl)tetrahydrofuran (0.050 mL, 0.5 mmol) and *N,N*-diisopropylamine (0.060 mL, 0.3
17
18 mmol) was added to a solution of **18** (110 mg, 0.33 mmol) in 1,2-dichloroethane (5 mL). The
19
20 mixture was heated to 80 °C for 20 h and then allowed to cool to room temperature. The reaction
21
22 mixture was poured into a saturated solution of sodium bicarbonate (5 mL). The organic layer
23
24 mixture was poured into a saturated solution of sodium bicarbonate (5 mL). The organic layer
25
26 was separated, dried (MgSO_4), filtered and concentrated. The residue was purified by silica gel
27
28 column chromatography (CH_2Cl_2 /methanol, 100/0–90/10) to afford 126 mg (92%) of **19** as a
29
30 yellow oil. MS (ES+) m/z 412 (M+H). ^1H NMR (400 MHz, CDCl_3) δ 8.25 (t, $J=4.6$ Hz, 1H),
31
32 8.12 (d, $J=8.8$ Hz, 1H), 7.47 (d, $J=8.0$ Hz, 2H), 7.33 (d, $J=8.0$ Hz, 2H), 6.95 (d, $J=1.4$ Hz, 1H),
33
34 6.76 (dd, $J=1.7, 8.9$ Hz, 1H), 4.10–4.19 (m, 1H), 3.98 (d, $J=13.3$ Hz, 1H), 3.88 (q, $J=7.8$ Hz, 1H),
35
36 3.74 (q, $J=7.8$ Hz, 1H), 3.60 (dd, $J=3.5, 11.1$ Hz, 1H), 3.29–3.48 (m, 4H), 2.92–3.01 (m, 1H),
37
38 2.71–2.80 (m, 1H), 2.29 (q, $J=7.80$ Hz, 1H), 1.59–2.07 (m, 8H).

39
40
41 **((R)-1-(4-(2-methyl-1-(((R)-tetrahydrofuran-2-yl)methyl)-1*H*-benzo[d]imidazol-6-**
42
43 **yl)benzyl)pyrrolidin-2-yl)methanol (20a).** Acetaldehyde (0.09 mL, 1.6 mmol) and sodium
44
45 hydrosulfite (84 mg, 0.48 mmol) were added to a solution of **19** (65 mg, 0.16 mmol) in a mixture
46
47 of ethanol (0.6 mL) and DMSO (0.15 mL). The mixture was heated at 80 °C for 18 h and then
48
49 allowed to cool to room temperature. The reaction mixture was diluted with EtOAc (4 mL) and
50
51 washed with brine (4 mL) followed by water (4 mL). The organic layer was dried (MgSO_4),
52
53
54
55
56
57
58
59
60

1
2
3 filtered and concentrated. The residue was dissolved in CH₂Cl₂ (4 mL) and trifluoroacetic acid
4
5 (5 drops) was added. The reaction mixture was stirred for 10 min and then concentrated. The
6
7 residue was purified by reverse-phase preparative HPLC to afford 10 mg (16%) of **20a**. MS
8
9 (ES+) *m/z* 406 (M+H). ¹H NMR (400 MHz, DMSO-*d*₆) δ 7.77 (s, 1H), 7.63 (d, J=8.1 Hz, 2H),
10
11 7.53 (d, J=8.4 Hz, 1H), 7.42 (d, J=9.5 Hz, 1H), 7.39 (d, J=8.1 Hz, 2H), 4.44 (br. s., 1H), 4.37 (d,
12
13 J=12.5 Hz, 1H), 4.26–4.14 (m, 3H), 4.07 (d, J=13.2 Hz, 1H), 3.75 (q, J=7.0 Hz, 1H), 3.61 (q,
14
15 J=7.0 Hz, 1H), 3.52–3.44 (m, 1H), 2.80 (br. s., 1H), 2.63–2.53 (m, 5H), 2.23–2.14 (m, 1H),
16
17 2.08–1.97 (m, 1H), 1.87–1.76 (m, 3H), 1.64–1.53 (m, 4H).
18
19
20
21

22 **Representative synthesis of compounds 22a-g.**

23
24 **4-((3-methyl-5-(phenylsulfonylmethyl)phenoxy)methyl)benzaldehyde (21).** A mixture of **6**
25 (500 mg, 1.91 mmol), 4-bromomethylbenzaldehyde (399 mg, 1.94 mmol), and potassium
26
27 carbonate (790 mg, 5.27 mmol) in acetonitrile (8 mL) was stirred at 60 °C for 2 hours. The
28
29 reaction mixture was diluted with EtOAc and 50% saturated aqueous sodium chloride. The
30
31 organic layer was washed with brine, dried (Na₂SO₄), and concentrated. The residue was
32
33 purified by silica gel chromatography (heptane/EtOAc, 9/1-1/1) to afford 684 mg (94%) of **21** as
34
35 a white solid. MS (ES+) *m/z* 381 (M+H).
36
37
38
39

40
41 **(R)-(1-(4-((3-methyl-5-(phenylsulfonylmethyl)phenoxy)methyl)benzyl)pyrrolidin-2-**
42
43 **yl)methanol (22a).** To a solution of (*R*)-(-)-2-pyrrolidinemethanol (147 mg, 1.44 mmol) in 1,2-
44
45 dichloroethane (6 mL) was sequentially added **21** (498 mg, 1.31 mmol) and sodium
46
47 triacetoxyborohydride (438 mg, 1.96 mmol). The reaction mixture was stirred at room
48
49 temperature overnight. The mixture was diluted with dichloromethane, washed with saturated
50
51 aqueous sodium bicarbonate. The organic layer was dried (Na₂SO₄), filtered, and concentrated.
52
53
54
55 The residue was purified by silica gel chromatography (CH₂Cl₂-CH₂Cl₂/methanol, 4/1) to afford
56
57
58
59
60

1
2
3 580 mg (95%) of **22a** as an oil. MS (ES+) m/z 466 (M+H). ^1H NMR (400 MHz, DMSO- d_6) δ
4 7.77–7.66 (m, 3 H), 7.64–7.54 (m, 2 H), 7.31 (s, 4 H), 6.77 (s, 1 H), 6.53 (s, 1 H), 6.51 (s, 1 H),
5 4.89 (s, 2 H), 4.56 (s, 2 H), 4.43 (br. s, 1 H), 4.04 (d, $J=13.2$ Hz, 1 H), 3.50–3.40 (m, 1 H), 3.36–
6 3.22 (m, 2 H), 2.83–2.69 (m, 1 H), 2.63–2.54 (m, 1 H), 2.17 (s, 3 H), 2.14–2.04 (m, 1 H), 1.92–
7 1.75 (m, 1 H), 1.67–1.48 (m, 3 H). Compound **22a** is commercially available via
8 MilliporeSigma (catalog # PZ0234). Compounds **22b-i** were prepared in a similar manner.
9
10
11
12
13
14

15 **1-Methoxy-3-((phenylsulfonyl)methyl)benzene (24a)**. NaSO₂Ph (2.46 g, 14.7 mmol) was
16 added to a solution of 1-(bromomethyl)-3-methoxybenzene **23** (2.0 mL, 14.0 mmol) in ethanol (7
17 mL) and the mixture was heated at 80 °C for 3.5 h. After cooling to room temperature, the
18 resulting precipitate was filtered and washed with water. The solid was dried under vacuum to
19 afford 3.25 g (89%) of **24a** as a white powder. MS (ES+) m/z 263 (M+H). ^1H NMR (400 MHz,
20 CDCl₃) δ ppm 7.64–7.69 (m, 2H), 7.63–7.57 (m, 1H), 7.50–7.42 (m, 2H), 7.15 (t, $J=7.9$ Hz, 1H),
21 6.88–6.82 (m, 1H), 6.68–6.62 (m, 1H), 6.61 (t, $J=2.1$ Hz, 1H), 4.28 (s, 2H), 3.70 (s, 3H).
22
23
24
25
26
27
28
29
30
31
32
33

34 Compounds **24b** and **24c** were prepared in a similar manner.
35

36 **3-((Phenylsulfonyl)methyl)phenol (25a)**. A solution of BBr₃ (1M in CH₂Cl₂, 12 mL, 12
37 mmol) was added to a solution of **24a** (1.5 g, 5.7 mmol) in CH₂Cl₂ (30 mL) at -20 °C and the
38 mixture was stirred for 1 h. The reaction mixture was quenched with a solution of 50% brine
39 and diluted with CH₂Cl₂. The aqueous phase was extracted with CH₂Cl₂. The combined organic
40 layers were dried (Na₂SO₄), filtered and concentrated to afford 1.41 g (95%) of **25a** as an off-
41 white solid. MS (ES+) m/z 249 (M+H). ^1H NMR (400 MHz, DMSO- d_6) δ 9.43 (s, 1H), 7.73–
42 7.68 (m, 2H), 7.60–7.56 (m, 2H), 7.05–7.01 (t, 1H), 6.69 (d, $J=7.8$, 1H), 6.62 (s, 1H), 6.51 (d,
43 $J=7.5$, 2H), 4.56 (s, 2H). Compounds **25b** and **25c** were prepared in a similar manner.
44
45
46
47
48
49
50
51
52
53
54
55
56
57
58
59
60

1
2
3
4
5
6
7
8
9
10
11
12
13
14
15
16
17
18
19
20
21
22
23
24
25
26
27
28
29
30
31
32
33
34
35
36
37
38
39
40
41
42
43
44
45
46
47
48
49
50
51
52
53
54
55
56
57
58
59
60

(R)-(1-(4-((3-((Phenylsulfonyl)methyl)phenoxy)methyl)benzyl)pyrrolidin-2-yl)methanol (26a). Compound **25a**, 4-bromomethylbenzaldehyde and (*R*)-(-)-2-pyrrolidinemethanol were reacted following the conditions described for compound **22a**. MS (ES+) *m/z* 452 (M+H). ¹H NMR (400 MHz, DMSO-*d*₆) δ 7.75–7.65 (m, 3H), 7.58 (t, *J*=7.7 Hz, 2H), 7.32 (br. s., 4H), 7.17 (t, *J*=7.9 Hz, 1H), 6.93 (dd, *J*=8.2, 2.0 Hz, 1H), 6.75 (s, 1H), 6.70 (d, *J*=7.7 Hz, 1H), 4.93 (s, 2H), 4.63 (s, 2H), 4.56–4.27 (m, 1H), 4.17–3.93 (m, 1H), 3.44 (br. s., 1H), 3.35–3.22 (m, 2H), 2.77 (br. s., 1H), 2.58 (br. s, 1H), 2.29–2.02 (m, 1H), 1.94–1.74 (m, 1H), 1.71–1.47 (m, 3H).

(R)-(1-(4-((3-((Cyclopropylsulfonyl)methyl)phenoxy)methyl)benzyl)pyrrolidin-2-yl)methanol (26b). Compound **25b**, 4-bromomethylbenzaldehyde and (*R*)-(-)-2-pyrrolidinemethanol were reacted following the conditions described for compound **22a**. MS (ES+) *m/z* 416 (M+H). ¹H NMR (600 MHz, DMSO-*d*₆) δ 7.43–7.34 (m, 4H), 7.32 (t, *J*=7.8 Hz, 1H), 7.10 (s, 1H), 7.04 (dd, *J*=8.2, 2.2 Hz, 1H), 7.02 (d, *J*=7.4 Hz, 1H), 5.10 (s, 2H), 4.48 (s, 2H), 4.46–4.34 (m, 1H), 4.08 (br. s., 1H), 3.48 (d, *J*=6.1 Hz, 1H), 2.81 (br. s., 1H), 2.20 (br. s., 1H), 1.87 (br. s., 1H), 1.72–1.55 (m, 3H), 0.96–0.84 (m, 4H).

(R)-(1-(4-((3-((Methylsulfonyl)methyl)phenoxy)methyl)benzyl)pyrrolidin-2-yl)methanol (26c). Compound **25c**, 4-bromomethylbenzaldehyde and (*R*)-(-)-2-pyrrolidinemethanol were reacted following the conditions described for compound **22a**. MS (ES+) *m/z* 390 (M+H). ¹H NMR (600 MHz, DMSO-*d*₆) δ 7.39 (d, *J*=7.7 Hz, 2H), 7.36–7.29 (m, 3H), 7.07 (s, 1H), 7.03 (dd, *J*=8.2, 2.2 Hz, 1H), 6.99 (d, *J*=7.7 Hz, 1H), 5.07 (s, 2H), 4.43 (s, 2H), 4.41–4.30 (m, 1H), 4.06 (d, *J*=11.0 Hz, 1H), 3.46 (d, *J*=7.1 Hz, 1H), 3.44–3.35 (m, 1H), 2.86 (s, 3H), 2.79 (br. s., 1H), 2.66–2.55 (m, 1H), 2.24–2.09 (m, 1H), 1.85 (br. s., 1H), 1.68–1.53 (m, 3H).

(R)-(1-(4-((3-cyclohexylphenoxy)methyl)benzyl)pyrrolidin-2-yl)methanol (27a). 3-Cyclohexylphenol, 4-bromomethylbenzaldehyde and (*R*)-(-)-2-pyrrolidinemethanol were reacted

1
2
3 following the conditions described for compound **22a**. MS (ES+) m/z 380 (M+H). ^1H NMR (400
4 MHz, CD_3OD) δ ppm 7.56–7.50 (m, 4H), 7.17 (t, $J=8.0$ Hz, 1H), 6.83–6.77 (m, 3H), 5.12 (s,
5 2H), 4.51 (d, $J=12.8$ Hz, 1H), 4.08 (d, $J=13.2$ Hz, 1H), 3.75–3.65 (m, 2H), 3.46 (s, 1H), 3.28–
6 3.24 (m, 1H), 3.05–3.03 (m, 1H), 2.47 (m, 1H), 2.20–2.14 (m, 1H), 2.03–2.00 (m, 1H), 1.93–
7 1.75 (m, 7H), 1.49–1.28 (m, 5H).

14
15 **(R)-(1-(4-((3-isopropylphenoxy)methyl)benzyl)pyrrolidin-2-yl)methanol (27b)**. 3-

16
17 Isopropylphenol, 4-bromomethylbenzaldehyde and (*R*)-(-)-2-pyrrolidinemethanol were reacted
18 following the conditions described for compound **22a**. MS (ES+) m/z 340 (M+H). ^1H NMR (400
19 MHz, CD_3OD) δ 7.62–7.56 (m, 4H), 7.25 (t, 8.0 Hz, 1H), 6.93–6.86 (m, 3H), 5.19 (s, 2H), 4.54
20 (d, $J=12.4$ Hz, 1H), 4.09 (d, $J=13.2$ Hz, 1H), 3.76–3.72 (m, 2H), 3.47–3.39 (m, 1H), 3.39–
21 3.31 (m, 1H), 3.04–2.90 (m, 2H), 2.25–2.23 (m, 1H), 2.06–1.93 (m, 3H), 1.31 (d, $J=7.2$ Hz, 6H).
22
23
24
25
26
27
28

29 **(R)-(1-(4-((3-(5-methyl-1,2,4-oxadiazol-3-yl)phenoxy)methyl)benzyl)pyrrolidin-2-**
30 **yl)methanol (27c)**. 3-(5-Methyl-1,2,4-oxadiazol-3-yl)phenol, 4-bromomethylbenzaldehyde and
31 (*R*)-(-)-2-pyrrolidinemethanol were reacted following the conditions described for compound
32 **22a**. MS (ES+) m/z 380 (M+H). ^1H NMR(400 MHz, CD_3OD) δ 7.66–7.54 (m, 6H), 7.45 (t, $J=8$
33 Hz, 1H), 7.20 (d, $J=6.8$ Hz, 1H), 5.24 (s, 2H), 4.55 (d, $J=12.8$ Hz, 1H), 4.12 (d, $J=13.2$ Hz, 1H),
34 3.78–3.67 (m, 2H), 3.53 (s, 1H), 3.33 (m, 1H), 3.11–3.09 (m, 1H), 2.67 (s, 3H), 2.22–2.20 (m,
35 1H), 2.06–2.03 (m, 1H), 1.96–1.91 (m, 2H).
36
37
38
39
40
41
42
43
44
45

46 **(R)-N-(3-((4-((2-(hydroxymethyl)pyrrolidin-1-yl)methyl)benzyl)oxy)phenyl)benzamide**
47 **(27d)**. *N*-(3-Hydroxyphenyl)benzamide, 4-bromomethylbenzaldehyde and (*R*)-(-)-2-
48 pyrrolidinemethanol were reacted following the conditions described for compound **22a**. MS
49 (ES+) m/z 417.5 (M+H). ^1H NMR (400 MHz, $\text{DMSO}-d_6$) δ 10.22 (s, 1H), 7.92 (d, $J=7.0$ Hz, 2H),
50 7.61–7.50 (m, 4H), 7.44–7.33 (m, 5H), 7.24 (t, $J=8.2$ Hz, 1H), 6.75 (dd, $J=8.1, 1.8$ Hz, 1H), 6.54
51
52
53
54
55
56
57
58
59
60

(s, 1H), 5.07 (s, 2H), 4.16 (br. s., 1H), 3.53–3.41 (m, 2H), 3.36 (br. s., 1H), 3.00–2.70 (m, 2H), 1.90 (br. s., 1H), 1.74–1.55 (m, 3H).

Pharmacology assays. FITC-S1P quantification employing the Caliper® assay, ADP quantification employing the Transcreener® assay, quantification of cellular C17-S1P formation, and isothermal titration calorimetry (ITC) were performed according to procedures previously described.³⁸ Quantitation of C17-S1P formation in human whole blood was performed according to procedures previously described.^{38,41}

ASSOCIATED CONTENT

Supporting Information. The Supporting Information is available free of charge on the ACS Publications website at DOI: 10.1021/acs.jmedchem.xxxxxxx.

Molecule formula strings (CSV)

Synthetic procedures and characterization data for analogs **20b-j** and **22b-i**. (PDF)

Kinome profiling for compounds **12**, **20a** and **22a**. (PDF)

AUTHOR INFORMATION

Corresponding Author

*Phone: +1-617-674-7362. E-mail: mark.e.schnute@pfizer.com

Notes

The authors declare no completing financial interest.

1
2
3
4
5
6
7
8
9
10
11
12
13
14
15
16
17
18
19
20
21
22
23
24
25
26
27
28
29
30
31
32
33
34
35
36
37
38
39
40
41
42
43
44
45
46
47
48
49
50
51
52
53
54
55
56
57
58
59
60
ACKNOWLEDGMENT

We thank Grace Munie for performing S1P receptor binding screens.

ABBREVIATIONS

ADP, adenosine diphosphate; CLP, caliper® assay format; DIBAL, diisobutylaluminum hydride; DIPEA, *N,N*-diisopropylethylamine; DMSO, dimethylsulfoxide; EtOAc, ethyl acetate; FITC, fluorescein isothiocyanate; GPCR, G protein-coupled receptor; LIPE, lipophilic ligand efficiency; MTT, 3-(4,5-dimethylthiazol-2-yl)-2,5-diphenyltetrazolium bromide; S1P, sphingosine-1-phosphate; SphK, sphingosine kinase; TFA, trifluoroacetic acid; THF, tetrahydrofuran; TS, Transcreener® assay format.

REFERENCES

1. Pitson, S. M. Regulation of sphingosine kinase and sphingolipid signaling. *Trends Biochem. Sci.* **2011**, *36*, 97–107.
2. Kim, R. H.; Takabe, K.; Milstien, S.; Spiegel, S. Export and functions of sphingosine-1-phosphate. *Biochim. Biophys. Acta* **2009**, *1791*, 692–696.
3. Pyne, S.; Adams, D. R.; Pyne, N. J. Sphingosine 1-phosphate and sphingosine kinases in health and disease: Recent advances. *Prog. Lipid Res.* **2016**, *62*, 93–106.
4. Proia, R. L.; Hla, T. Emerging biology of sphingosine-1-phosphate: its role in pathogenesis and therapy. *J. Clin. Invest.* **2015**, *125*, 1379–1387.
5. Maceyka, M.; Spiegel, S. Sphingolipid metabolites in inflammatory disease. *Nature* **2014**, *510*, 58–67.

- 1
2
3 6. Melendez, A. J.; Carlos-Dias, E.; Gosink, M.; Allen, J. M.; Takacs, L. Human
4 sphingosine kinase: Molecular cloning, functional characterization and tissue distribution. *Gene*
5
6 **2000**, *251*, 19–26.
7
8
9
10
11 7. Liu, H.; Sugiura, M.; Nava, V. E.; Edsall, L. C.; Kono, K.; Poulton, S.; Milstien, S.;
12 Kohama, T.; Spiegel, S. Molecular cloning and functional characterization of a novel
13 mammalian sphingosine kinase type 2 isoform. *J. Biol. Chem.* **2000**, *275*, 19513–19520.
14
15
16
17
18
19 8. Allende, M. L.; Sasaki, T.; Kawai, H.; Olivera, A.; Mi, Y.; Van Echten-Deckert, G.;
20 Hajdu, R.; Rosenbach, M.; Keohane, C. A.; Mandala, S.; Spiegel, S.; Proia, R. L.; Mice deficient
21 in sphingosine kinase 1 are rendered lymphopenic by FTY720. *J. Biol. Chem.* **2004**, *279*, 52487–
22 52492.
23
24
25
26
27
28
29 9. Mizugishi, K.; Yamashita, T.; Olivera, A.; Miller, G. F.; Spiegel, S.; Proia, R. L.
30 Essential role for sphingosine kinases in neural and vascular development. *Mol. Cell. Biol.* **2005**,
31 *25*, 11113–11121.
32
33
34
35
36
37 10. Zemann, B.; Kinzel, B.; Müller, M.; Reuschel, R.; Mechtcheriakova, D.; Urtz, N.;
38 Bornancin, F.; Baumruker, T.; Billich, A. Sphingosine kinase type 2 is essential for lymphopenia
39 induced by the immunomodulatory drug FTY720. *Blood* **2006**, *107*, 1454–1458.
40
41
42
43
44
45 11. Sensken, S.-C.; Bode, C.; Nagarajan, M.; Peest, U.; Pabst, O.; Gräler, M. H..
46 Redistribution of sphingosine 1-phosphate by sphingosine kinase 2 contributes to lymphopenia.
47 *J. Immunol.* **2010**, *184*, 4133–4142.
48
49
50
51
52
53
54
55
56
57
58
59
60

1
2
3
4
5
6
7
8
9
10
11
12
13
14
15
16
17
18
19
20
21
22
23
24
25
26
27
28
29
30
31
32
33
34
35
36
37
38
39
40
41
42
43
44
45
46
47
48
49
50
51
52
53
54
55
56
57
58
59
60

12. Kharel, Y.; Raje, M.; Gao, M.; Gellett, A. M.; Tomsig, J. L.; Lynch, K. R.; Santos, W. L. Sphingosine kinase type 2 inhibition elevates circulating sphingosine 1-phosphate. *Biochem. J.* **2012**, *447*, 149–157.

13. Brinkmann, V.; Lynch, K. R. FTY720: targeting G-protein-coupled receptors for sphingosine 1-phosphate in transplantation and autoimmunity. *Curr. Opin. Immunol.* **2002**, *14*, 569–575.

14. Budde, K.; Schmouder, R. L.; Brunkhorst, R.; Nashan, B.; Lücker, P. W.; Mayer, T.; Choudhury, S.; Skerjanec, A.; Kraus, G.; Neumayer, H. H. First human trial of FTY720, a novel immunomodulator, in stable renal transplant patients. *J. Am. Soc. Nephrol.* **2002**, *13*, 1073–1083.

15. Sanford, M. Fingolimod: A review of its use in relapsing-remitting multiple sclerosis. *Drugs* **2014**, *74*, 1411–1433.

16. Baker, D. A.; Barth, J.; Chang, R.; Obeid, L. M.; Gilkeson, G. S. Genetic sphingosine kinase 1 deficiency significantly decreases synovial inflammation and joint erosions in murine TNF- α -induced arthritis. *J. Immunol.* **2010**, *185*, 2570–2579.

17. Baker, D. A.; Eudaly, J.; Smith, C. D.; Obeid, L. M.; Gilkeson, G. S. Impact of sphingosine kinase 2 deficiency on the development of TNF-alpha-induced inflammatory arthritis. *Rheumatol. Int.* **2013**, *33*, 2677–2681.

18. Snider, A. J.; Kawamori, T.; Bradshaw, S. G.; Orr, K. A.; Gilkeson, G. S.; Hannun, Y. A.; Obeid, L. M. A role for sphingosine kinase 1 in dextran sulfate sodium-induced colitis. *FASEB J.* **2009**, *23*, 143–152.

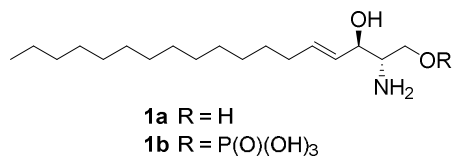
- 1
2
3
4
5
6
7
8
9
10
11
12
13
14
15
16
17
18
19
20
21
22
23
24
25
26
27
28
29
30
31
32
33
34
35
36
37
38
39
40
41
42
43
44
45
46
47
48
49
50
51
52
53
54
55
56
57
58
59
60
19. Huang, L. S.; Natarajan, V. Sphingolipids in pulmonary fibrosis. *Adv. Biol. Regul.* **2015**, *57*, 55–63.
20. Huang, L. S.; Berdyshev, E.; Mathew, B.; Panfeng Fu, P.; Gorshkova, I. A.; He, D.; Ma, W.; Noth, I.; Ma, S-F.; Pendyala, S.; Reddy, S. P.; Zhou, T.; Zhang, W.; Garzon, S. A.; Garcia, J. G. N.; Natarajan, V. Targeting sphingosine kinase 1 attenuates bleomycin-induced pulmonary fibrosis. *FASEB J.* **2013**, *27*, 1749–1760.
21. Geng, T.; Sutter, A.; Harland, M. D.; Law, B. A.; Ross, J. S.; Lewin, D.; Palanisamy, A.; Russo, S. B.; Chavin, K. D.; Cowart, L. A. SphK1 mediates hepatic inflammation in a mouse model of NASH induced by high saturated fat feeding and initiates proinflammatory signaling in hepatocytes. *J. Lipid Res.* **2015**, *56*: 2359–2371.
22. Yaghobian, D.; Don, A. D.; Yaghobian, S.; Chen, X.; Pollock, C. A.; Saad, S. Increased sphingosine 1-phosphate mediates inflammation and fibrosis in tubular injury in diabetic nephropathy. *Clin. Exp. Pharmacol. Physiol.* **2016**, *43*, 56–66.
23. Zhang, F.; Xia, Y.; Yan, W.; Zhang, H.; Zhou, F.; Zhao, S.; Wang, W.; Zhu, D.; Xin, C.; Lee, Y.; Zhang, L.; He, Y.; Gao, E.; Tao, L. Sphingosine 1-phosphate signaling contributes to cardiac inflammation, dysfunction, and remodeling following myocardial infarction. *Am. J. Physiol. Heart Circ. Physiol.* **2016**, *310*, H250–H261.
24. MacRitchie, N.; Volpert, G.; Washih, M. A.; Watson, D. G.; Futerman, A. H.; Kennedy, S.; Pyne, S.; Pyne, N. J. Effect of the sphingosine kinase 1 selective inhibitor, PF-543 on arterial and cardiac remodelling in a hypoxic model of pulmonary arterial hypertension. *Cell. Signalling* **2016**, *28*, 946–955.

- 1
2
3 25. Zhang, Y.; Wang, Y.; Wan, Z.; Liu, S.; Cao, Y.; Zeng, Z. Sphingosine kinase 1 and
4 cancer: A systematic review and meta-analysis. *PLoS ONE* **2014**, *9*, e90362.
5
6
7
8
9 26. Heffernan-Stroud, L. A.; Obeid, L. M. Sphingosine kinase 1 in cancer. *Adv. Cancer Res.*
10 **2013**, *117*, 201–235.
11
12
13
14 27. Newton, J.; Lima, S.; Maceyka, M; Spiegel, S. Revisiting the sphingolipid rheostat:
15 Evolving concepts in cancer therapy. *Exp. Cell Res.* **2015**, *333*, 195–200.
16
17
18
19
20 28. Rex, K.; Jeffries, S. J.; Brown, M. L.; Carlson, T.; Coxon, A.; Fajardo, F.; Frank, B.;
21 Gustin, D.; Kamb, A.; Kassner, P. D.; Li, S.; Li, Y.; Morgenstern, K.; Plant, M.; Quon, K.;
22 Ruefli-Brasse, A.; Schmidt, J.; Swearingen, E.; Walker, N.; Wang, Z.; Watson, J. E. V.;
23 Wickramasinghe, D.; Wong, M.; Xu, G.; Wesche, H. Sphingosine kinase activity is not required
24 for tumor cell viability. *PLoS ONE* **2013**, *8*, e68328.
25
26
27
28
29
30
31
32
33 29. Zhang, Y.; Berka, V.; Song, A.; Sun, K.; Wang, W.; Zhang, W.; Ning, C.; Li, C.; Zhang,
34 Q.; Bogdanov, M.; Alexander, D. C.; Milburn, M. V.; Ahmed, M. H.; Lin, H.; Idowu, M.;
35 Zhang, J.; Kato, G. J.; Abdulmalik, O. Y.; Zhang, W.; Dowhan, W.; Kellems, R. E.; Zhang, P.;
36 Jin, J.; Safo, M.; Tsai, A-L.; Juneja, H. S.; Xia, Y. Elevated sphingosine-1-phosphate promotes
37 sickling and sickle cell disease progression. *J. Clin. Invest.* **2014**, *124*, 2750–2761.
38
39
40
41
42
43
44
45
46 30. Plano, D.; Amin, S.; Sharma, A. K. Importance of sphingosine kinase (SphK) as a target
47 in developing cancer therapeutics and recent developments in the synthesis of novel SphK
48 inhibitors. *J. Med. Chem.* **2014**, *57*, 5509–5524.
49
50
51
52
53
54 31. Santos, W. L.; Lynch, K. R. Drugging sphingosine kinases. *ACS Chem. Biol.* **2015**, *10*,
55 225–233.
56
57
58
59
60

- 1
2
3 32. Pitman, M. R.; Costabile, M.; Pitson, S. M. Recent advances in the development of
4 sphingosine kinase inhibitors. *Cell. Signalling* **2016**, *28*, 1349–1363.
5
6
7
8
9 33. Xiang, Y.; Hirth, B.; Kane, J. L., Jr.; Liao, J.; Noson, K. D.; Yee, C.; Asmussen, G.;
10 Fitzgerald, M.; Klaus, C.; Booker, M. Discovery of novel sphingosine kinase-1 inhibitors. Part 2.
11
12 *Bioorg. Med. Chem. Lett.* **2010**, *20*, 4550–4554.
13
14
15
16
17 34. Gustin, D. J.; Li, Y.; Brown, M. L.; Min, X.; Schmitt, M. J.; Wanska, M.; Wang, X.;
18 Connors, R.; Johnstone, S.; Cardozo, M.; Cheng, A. C.; Jeffries, S.; Franks, B.; Li, S.; Shen, S.;
19 Wong, M.; Wesche, H.; Xu, G.; Carlson, T. J.; Plant, M.; Morgenstern, K.; Rex, K.; Schmitt, J.;
20
21 Coxon, A.; Walker, N.; Kayser, F.; Wang, Z. Structure guided design of a series of sphingosine
22
23 kinase (SphK) inhibitors. *Bioorg. Med. Chem. Lett.* **2013**, *23*, 4608–4616.
24
25
26
27
28
29
30 35. Patwardhan, N. N.; Morris, E. A.; Kharel, Y.; Raje, M. R.; Gao, M.; Tomsig, J. L.;
31 Lynch, K. R.; Santos, W. L. Structure–activity relationship studies and in vivo activity of
32
33 guanidine-based sphingosine kinase inhibitors: Discovery of SphK1- and SphK2-selective
34
35 inhibitors. *J. Med. Chem.* **2015**, *58*, 1879–1899.
36
37
38
39
40 36. Houck, J. D.; Dawson, T. K.; Kennedy, A. J.; Kharel, Y.; Naimon, N. D.; Field, S. D.;
41 Lynch, K. R.; Macdonald, T. L. Structural requirements and docking analysis of amidine-based
42
43 sphingosine kinase 1 inhibitors containing oxadiazoles. *ACS Med. Chem. Lett.* **2016**, *7*, 487–492.
44
45
46
47
48 37. Congdon, M. D.; Kharel, Y.; Brown, A. M.; Lewis, S. N.; Bevan, D. R.; Lynch, K. R.;
49 Santos, W. L. Structure–activity relationship studies and molecular modeling of naphthalene-
50
51 based sphingosine kinase 2 inhibitors. *ACS Med. Chem. Lett.* **2016**, *7*, 229–234.
52
53
54
55
56
57
58
59
60

- 1
2
3 38. Schnute, M. E.; McReynolds, M. D.; Kasten, T.; Yates, M.; Jerome, G.; Rains, J. W.;
4 Hall, T.; Chrencik, J.; Kraus, M.; Cronin, C. N.; Saabye, M.; Highkin, M. K.; Broadus, R.;
5 Ogawa, S.; Cukyne, K.; Zawadzke, L. E.; Peterkin, V.; Iyanar, K.; Scholten, J. A.; Wendling, J.;
6 Fujiwara, H.; Nemirovskiy, O.; Wittwer, A. J.; Nagiec, M. M. Modulation of cellular S1P levels
7 with a novel, potent and specific inhibitor of sphingosine kinase-1. *Biochem. J.* **2012**, *444*, 79–
8 88.
9
10
11
12
13
14
15
16
17
18 39. Hawkins, P. C. D.; Skillman, A. G.; Nicholls, A. Comparison of shape-matching and
19 docking as virtual screening tools. *J. Med. Chem.* **2007**, *50*, 74–82.
20
21
22
23
24 40. Compound **22a** is commercially available via MilliporeSigma (catalog # PZ0234).
25
26
27 41. Highkin, M. K.; Yates, M. P.; Nemirovskiy, O. V.; Lamarr, W. A.; Munie, G. E.; Rains,
28 J. W.; Masferrer, J. L.; Nagiec, M. M. High-throughput screening assay for sphingosine kinase
29 inhibitors in whole blood using RapidFire® mass spectrometry. *J. Biomol. Screen.* **2011**, *16*,
30 272–277.
31
32
33
34
35
36
37 42. Wang, J.; Knapp, S.; Pyne, N. J.; Pyne, S.; Elkins, J. M. Crystal structure of sphingosine
38 kinase 1 with PF-543. *ACS Med. Chem. Lett.* **2014**, *5*, 1329–1333.
39
40
41
42
43 43. Baell, J. B.; Holloway, G. A. New substructure filters for removal of pan assay
44 interference compounds (PAINS) from screening libraries and for their exclusion in bioassays. *J.*
45 *Med. Chem.* **2010**, *53*, 2719–2740.
46
47
48
49
50
51 44. Newman, M. S.; Landers, J. O. Cycliacylation studies on 3,5-disubstituted
52 phenylalkanoic acids. *J. Org. Chem.* **1977**, *42*, 2556–2559.
53
54
55
56
57
58
59
60

TABLES AND FIGURES

Figure 1. Sphingosine (**1a**) and sphingosine-1-phosphate (S1P, **1b**).

1
2
3
4
5
6
7 **Figure 2.** Inhibitors of SphK1 and SphK2.
8
9

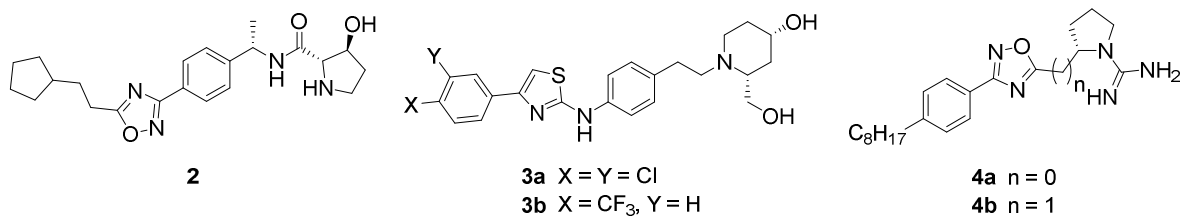


Figure 3. SphK1 screening hits. Fragments for combination shown in blue.

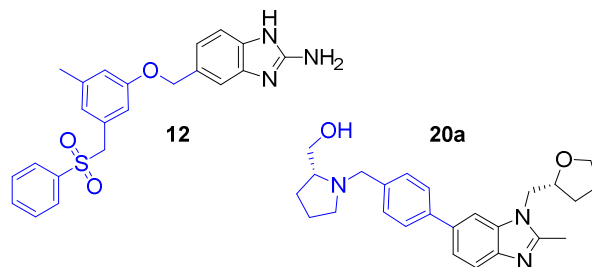


Figure 4. Correlation of cellular C17-S1P inhibition to SphK1 enzyme inhibition for benzylpyrrolidine series. black solid line, linear data fit; red dashed lines, boundary for 2-fold deviation from ideal correlation.

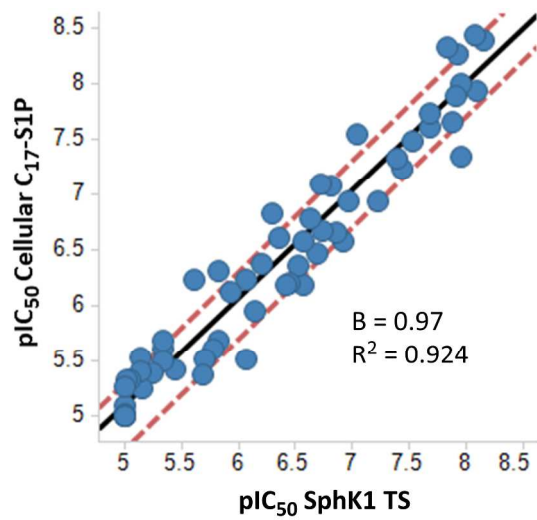


Figure 5. ROCS alignment of compounds **12** (A) and **20a** (B). Connolly surface represents polar regions (green) and hydrophobic regions (orange).

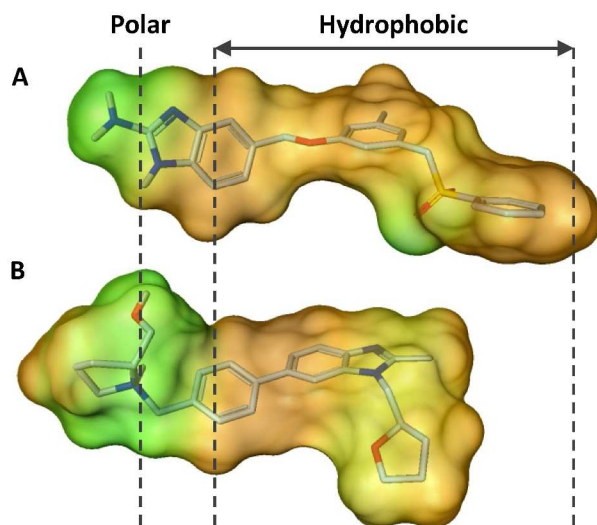
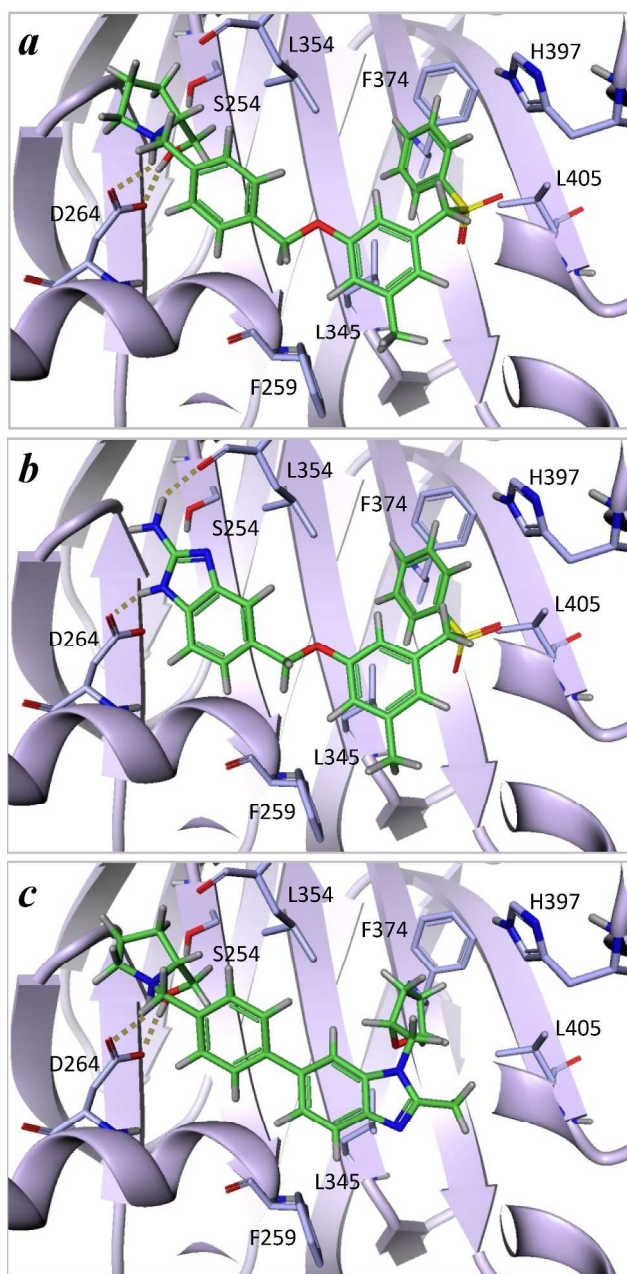
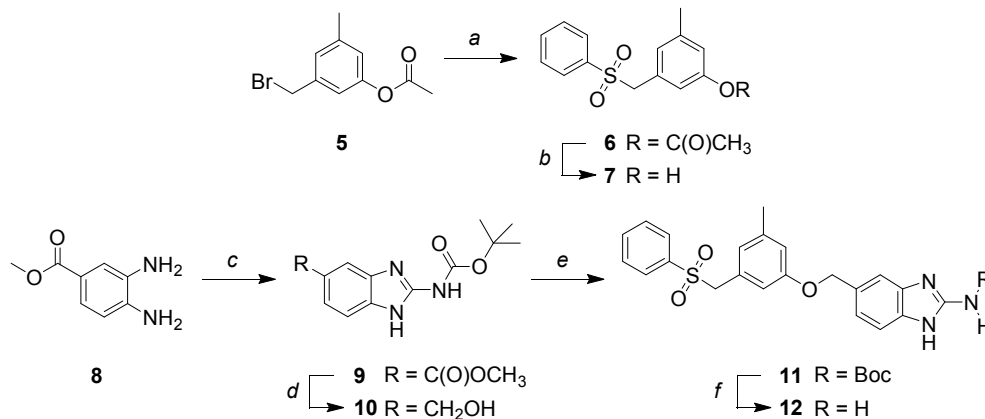
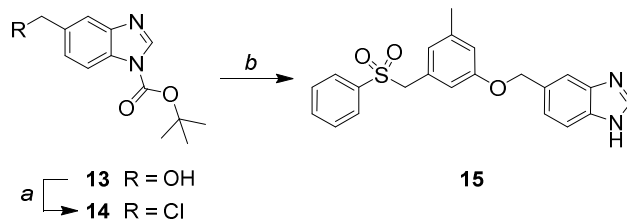


Figure 6. Binding modes of SphK1 inhibitors: (a) Compound **22a** bound to SphK1 as described in the reported co-crystal structure (PDB 4V24).⁴² (b and c) Proposed bound conformations of compounds **12** and **20a** based on docking (AGDOCK) of ligands to the SphK1 protein structure reported in PDB 4V24.

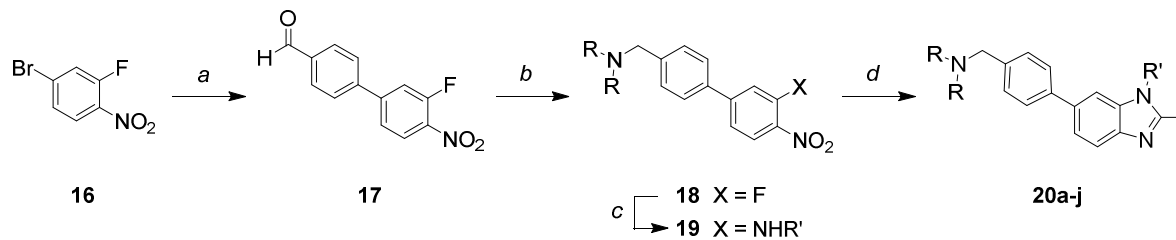


Scheme 1. Synthesis of screening hit **12**^a

^aReagents and conditions: (a) NaSO₂Ph, Aliquat® 336, 85 °C; (b) Na₂CO₃, methanol/water; (c) 1,3-bis(*tert*-butoxycarbonyl)-2-methyl-2-thioseourea, methanol, reflux; (d) DIBAL, CH₂Cl₂, -78 °C; (e) **7**, PS-PPh₃, di-*tert*-butyl azodicarboxylate, THF; (f) TFA, CH₂Cl₂.

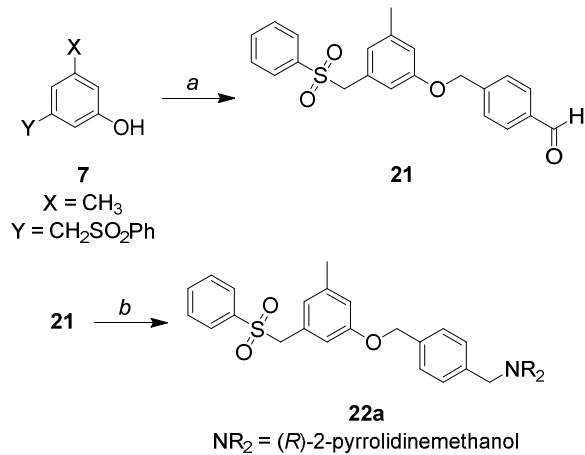
Scheme 2. Synthesis of compound **15**^a

^aReagents and conditions: (a) PS-Ph₃P, CCl₄; (b) **7**, K₂CO₃, acetone, 65 °C; TFA, CH₂Cl₂.

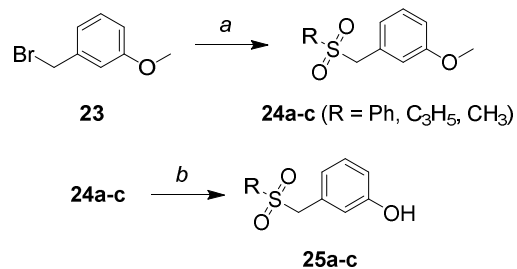
Scheme 3. General synthesis of benzimidazoles **20a-j**^a

^aReagents and conditions: (a) (4-formylphenyl)boronic acid, 2-(dicyclohexylphosphino)-biphenyl, Pd(OAc)₂, KF, dioxane, 65 °C; (b) NaBH(OAc)₃, (*R*)/(*S*)-2-(hydroxymethyl)pyrrolidine or pyrrolidine, 1,2-dichloroethane; (c) H₂NR', DIPEA, 1,2-dichloroethane, 80 °C; (d) acetaldehyde, Na₂S₂O₄, ethanol/DMSO; TFA, CH₂Cl₂.

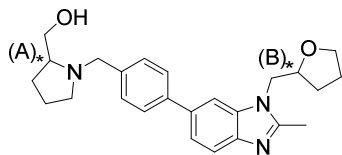
Scheme 4. Representative synthesis of aryether amines **22a-g**, **26a-c** and **27a-d**^a



^aReagents and conditions: (a) 4-bromomethylbenzaldehyde, K₂CO₃, acetonitrile, 60 °C; b) (*R*)-2-pyrrolidinemethanol, NaBH(OAc)₃, 1,2-dichloroethane.

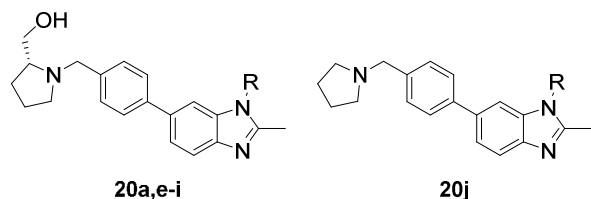
Scheme 5. Synthesis of phenols **25a-c**^a

^aReagents and conditions: (a) NaSO_2R , ethanol, $80\text{ }^\circ\text{C}$; (b) BBr_3 , CH_2Cl_2 .

Table 1. Pharmacology for benzylpyrrolidine diastereomers **20a-d**^a

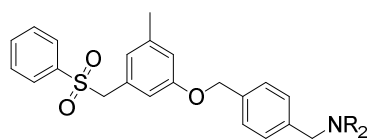
Compound	Config (A,B)	SphK1 IC ₅₀ (μM)			SphK2 IC ₅₀ (μM) CLP	SphK1 ITC K _d (μM)
		TS	C ₁₇ -S1P	CLP		
20a	(<i>R,R</i>)	0.19	0.081	0.87	46	2.9
20b	(<i>R,S</i>)	4.6	2.1	12.7	>100	12
20c	(<i>S,R</i>)	31	9.8	>100	>100	ND
20d	(<i>S,S</i>)	>100	>100	>100	>100	ND

^aAll values are the mean of two or more independent assays. ND, not determined; TS, Transcreener® (ADP formation) enzyme assay format; CLP, Caliper® (FITC-S1P formation) enzyme assay format; C17-S1P, C17-S1P formation in 1483 head and neck carcinoma cells.

Table 2. SAR of benzylpyrrolidine series^a

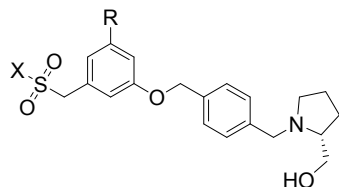
Compound	R	SphK1 IC ₅₀ (μM)		LIPE ^b
		TS	C17-S1P	
20a	(<i>R</i>)-(tetrahydrofuran-2-yl)methyl	0.19	0.081	4.8
20e	cyclobutylethyl	0.008	0.004	4.4
20f	isopentyl	0.007	0.004	4.5
20g	cyclopentylmethyl	0.011	0.010	4.0
20h	benzyl	0.44	0.25	2.8
20i	isobutyl	0.29	0.44	2.9
20j	(<i>R</i>)-(tetrahydrofuran-2-yl)methyl	>100	ND	ND

^aAll values are the mean of two or more independent assays. ^bCalculated based on cellular C17-S1P potency and cLogD (ACD version 12). ND, not determined; TS, Transcreener® (ADP formation) enzyme assay format; C17-S1P, C17-S1P formation in 1483 head and neck carcinoma cells.

Table 3. SAR for hydroxylamine substituent in arylether amines **22a-g**^a

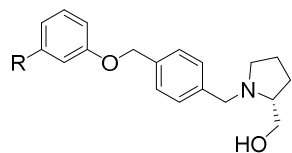
Compound	NR ₂	SphK1 IC ₅₀ (nM)			SphK2	HWB
		TS	C ₁₇ -S1P	CLP	IC ₅₀ (nM) CLP	S1P IC ₅₀ (nM)
22a		2.0	0.8	2.7	356	20
22b		78	43	142	42,600	703
22c		3.0 ^b	0.03	2.6 ^b	443	5.2
22d		28	30	ND	ND	ND
22e		2.0 ^b	0.17	2.0 ^b	465	6.4
22f		3.9	1.0	3.9	7,230	38
22g		5.3	3.5	14.6	35,100	ND

^aAll values are the mean of two or more independent assays. ^bCompound potency may exceed dynamic range of assay. ND, not determined; TS, Transcreener® (ADP formation) enzyme assay format; CLP, Caliper® (FITC-S1P formation) enzyme assay format; C₁₇-S1P, C₁₇-S1P formation in 1483 head and neck carcinoma cells; HWB, human whole blood.

Table 4. SAR for tail region in aryloether amines **26a-c**^a

Compound	R	X	SphK1 IC ₅₀ (nM)			SphK2 IC ₅₀ (nM) CLP	HWB S1P IC ₅₀ (nM)
			TS	C ₁₇ -S1P	CLP		
22a	Me	Ph	2.0	0.8	2.7	356	20
26a	H	Ph	2.0	0.3	2.4	164	35
26b	H	C ₃ H ₅	10	1.7	40.4	164	1,470
26c	H	CH ₃	439	519	ND	ND	ND

^aAll values are the mean of two or more independent assays. ND, not determined; TS, Transcreener® (ADP formation) enzyme assay format; CLP, Caliper® (FITC-S1P formation) enzyme assay format; C17-S1P, C17-S1P formation in 1483 head and neck carcinoma cells; HWB, human whole blood.

Table 5. Pharmacology of SphK1/2 dual and SphK2 preferential inhibitors **27a-d**^a

Compound	R	SphK1 IC ₅₀ (nM)			SphK2	HWB
		TS	C ₁₇ -S1P	CLP	IC ₅₀ (nM) CLP	S1P IC ₅₀ (nM)
27a	chex	0.7 ^b	0.03	<1.7	<1.7	1.5
27b	iPr	0.8	0.6	4.8	<1.7	19
27c		4.5	1.7	25	2.4	173
27d	NHC(O)Ph	3,670	1,200	9,820	145	>8,800

^aAll values are the mean of two or more independent assays. ^bCompound potency may exceed dynamic range of assay. ND, not determined; TS, Transcreener® (ADP formation) enzyme assay format; CLP, Caliper® (FITC-S1P formation) enzyme assay format; C₁₇-S1P, C₁₇-S1P formation in 1483 head and neck carcinoma cells; HWB, human whole blood.

Table of Contents Graphic

